كلية الهندسة بشبرا
FACULTY OF ENGINEERING AT SHOUBRA
ERJ
PRINT ISSN 3009-6049
ONLINE ISSN 3009-6022

ENGINEERING RESEARCH JOURNAL (ERJ)
Volume (53),Issue (3)
July 2024, pp:113-124
https://erjsh.journals.ekb.eg

Upgrading the load-carrying capacity of old riveted steel bridge – Case study

A.M. Anwar

Construction Research Institute, National Water Research Center, Cairo, 12631
E-mail address: ahmed_anwar@nwrc.gov.eg

Abstract: This paper describes a comprehensive structural assessment of a heritage riveted steel bridge laying over a navigation lock. This bridge was constructed over 135 years ago and is in service till now. The bridge was subjected to severe deterioration due to aging problems. The challenge was to set up an intensive rehabilitation program while increasing the bridge's load-carrying capacity to accommodate new heavy traffic loads. Site inspections were conducted for the original bridge structural and mechanical parts. The structural performance was evaluated using dynamic and static in-situ tests. Eight accelerometers were mounted and distributed across the bridge area. Modal analysis was conducted before and after strengthening. The strain was also recorded at the end of the retrofitting process. The concept of strengthening was to create a stiffer structural system capable of decreasing the stress level on the old system. Additional thermal stresses caused by extensive welding, especially for the main riveted girders, were avoided during the strengthening program. Moreover, the original bracing system was kept without removing any of its elements. Plane trusses were constructed to carry the bridge along secondary hot-rolled beams. The trusses were connected laterally through horizontal and inclined members. The structural rigidity was evaluated after strengthening. The fundamental natural frequency of the bridge was enhanced by 38%. This research depicts the successful efforts for upgrading a heritage bridge without affecting its original riveted components.

Keywords: Riveted steel bridges; Dynamic measurements; Strain measurements; Strengthening; Fatigue cracks.

1. Introduction

Retrofitting of heritage hydraulic structures is crucial to keep them in normal hydraulic operation while bearing service traffic loads. Nevertheless, the increasing demands for upgrading road capacities make the matter more complicated as all structural elements should be checked even if no signs of deterioration are observed. On the other hand, the total replacement of these structures can cost a lot. Additionally, it is time-consuming. The current research represented a case study for upgrading of Gamgara barrage. The barrage is located in Banha – Egypt, and particularly at KM 3.650 along the Tawfiki Canal. The barrage was constructed from masonry and was built in 1885. The regulator consists of five hydraulic vents in addition to an attached navigation lock. It was intended to upgrade the regulator and raise its load-carrying capacity from 20 to 60 Ton along with the necessary repair works. A movable built-up riveted steel bridge - overlaying a navigation lock of 8.00 m width - was considered in this research.

A review article [1] stated that fatigue, corrosion, and bolt loosening are the main causes of structural performance degradation as well as the collapse of steel bridges. Other problems have been addressed for centenary steel bridges [2] such as severe corrosion, delamination and defoliation at section edges, localized deformation of section plates at the riveted connections, deterioration of bearing pads, and severe degradation of asphaltic layers. Alternatively, fatigue assessment is often not an easy task, especially when the bridge is suffering from some sort of fatigue cracks and overall deterioration features [3,4].

Strengthening of aged steel bridges either welded or riveted is of great concern to many researchers [5-9]. The idea of the reuse concept rather than demolishing and replacement can give the structure a second life for sustainable development [4,10]. It was stated that the undertaken rehabilitation for centenarian steel bridges can be summarized as any/some of the following: straightening of steel elements, restoration of connection joints, pickling of some plates, replacement of rivets with new ones to respect aesthetics and original design, and repositioning of support devices and bearings [11]. Mash et. al [12] made a comparison between different repairing techniques such as bolting, making concrete encasement, and using externally bonded fiber-reinforced polymers (FRP). It was concluded that despite extensive mechanical and chemical surface preparation, the bond of the FRP system to a damaged substrate metallic surface was poor. An efficient prestressing technique using bonded iron-based shape memory alloy (Fe-SMA) to strengthen cracked U-rib buttwelded joints proactively was proposed [13], [14]. Pre-stressing of metallic bridges using Carbon Fiber Reinforced Polymers (CFRP) plates was also examined by many researchers [15], [16].

It was stated that the detection of hidden cracks in riveted joints is difficult; X-ray inspection requires complex precautions while ultrasonic tests are very expensive [17]. A structural health monitoring and restoration program of riveted steel arch bridge was previously studied [18], the study monitored the ambient vibrations and dynamic characteristics of the bridge were obtained. Moreover, continuous field static and dynamic measurements to predict

the failure scenarios of steel railway truss bridges were performed [19] where local failures can be identified using vertical deflections and modal frequencies. Barros et. al [20] adopted a model-based decision tree algorithm for the routine inspection of steel bridges based on actual measured modal properties. Stress distribution near the vicinity of rivet holes as well as crack propagation in riveted single shear lap joints under cyclic loading were focused [21]. Numerical modelling also played an important role in simulating the real behavior of existing structures as well as estimating their performance after strengthening or repair works [22], [23].

The current research focuses on rehabilitating and strengthening of a movable single-leaf double-beam roadway drawbridge (bascule bridge). The retrofitting included treatment of corrosion, cracks, delamination, and changing the deteriorated bearings that were noticed during field inspection. The challenge was therefore to undergo the strengthening works without having any negative effects on the original riveted built-up steel sections. The strengthening program, is therefore, intended to avoid any thermal stresses resulting from the welding process and might affect the tightness of the existing rivets. Thus, a truss system was proposed to be attached to the existing bridge from underneath. The combined system, the old bridge along with the new truss, was capable of carrying most of the applied loads and consequently, releasing the high stresses generated among the original deteriorated steel sections of the bridge. This would have better efficiency in upgrading the entire system rather than strengthening each single member alone. Numerical modeling was conducted as well. Evaluation took place using dynamic evaluation before and after retrofitting. Additionally, dynamic strain measurements were recorded during normal operational traffic loads to capture the working strain levels and ensure the mitigation of the structural integrity of the bridge.

2. BRIDGE DESCRIPTION

The steel bridge is a movable single-leaf drawbridge that depends on a counter mass for the opening process. The bridge overlays a navigation lock of 8.00 m in width. The bridge is a part of Gamgara's old regulator that is still in service up to date. Figure (1) shows the elevation view for the regulator and attached bridge from downstream side – captured from original design drawings at the owner's archive. The bridge rests on a masonry abutment from one side while the other side is also a masonry guide wall. Figure (2) shows a photo of the bridge from the upstream side. The bridge is composed of mainly three built-up girders connected using rivets and has a total depth of 620 mm. The bridge also has two built-up cross girders, 600 mm depth, at 1/3 and 2/3 of the bending span. At the time of opening, the bridge is hung from the ends of one of these two cross girders. The system of the main girders is connected at the edges using an end beam that transfers the superimposed loads directly to the abutments through three bearings at each side. Additionally, four secondary beams of hot rolled sections, IPE 300, are arranged in between the main girders at equal distances. This group of beams is overlaid by a grid system of stringers spacing 500 mm in the main bridge direction and 300 mm in the opposite direction. The stringers' sections are hot rolled sections of sections IPE140, and IPE200 arranged along main and perpendicular bridge directions, respectively. The bridge is braced using angles 70x7 riveted to the main girders through gusset plates. The bridge's clear width was originally 8.0 m with two sidewalks each of 650 mm width. Figure (3) shows a real photo of the arrangement of the sleepers during removal for repair. The sleepers are covered using a steel plate of 12 mm thickness and finally overlaid with approximately 20 mm asphaltic layer.

3. REHABILITATION PROGRAM

At the beginning, intensive field inspection was conducted. The inspection included checking all bridge components as well as its bearings. Focus was given to the condition of rivets where few numbers were subjected to tearing or loosening of tightness due to severe corrosion at some parts. Local bending and tearing of some sections were also noticed. The Lamination phenomenon and intensive corrosion were observed at the end girders where these sections were fully embedded in backfilled soil that caused coating delamination. The bearings were also deteriorated and are in deep need of replacement. The mechanical system for lifting also malfunctioned, and the bridge was not moving anymore. Figure (5) shows some figures of bridge deterioration.

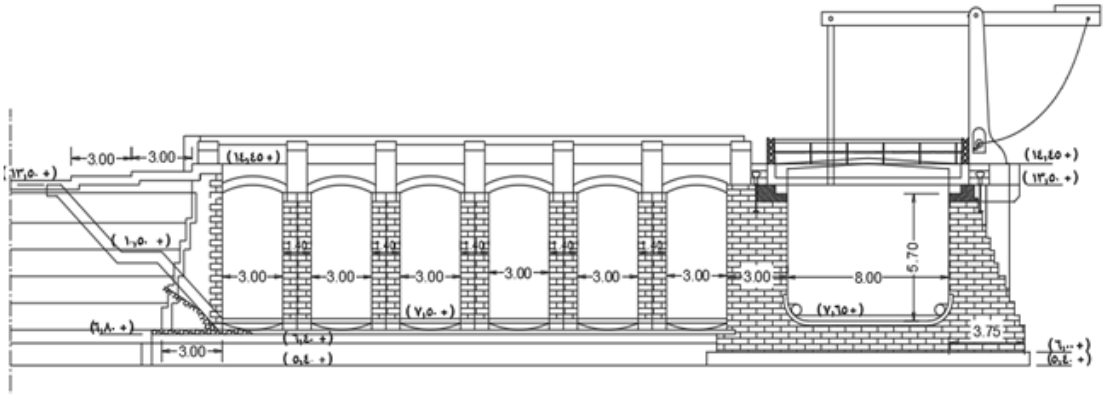

FIGURE 1. Elevation showing, regular, navigation lock, and the steel bridge [original Design Drawings, 1888]

FIGURE 2. General view of the steel bridge before rehabilitation

(a)

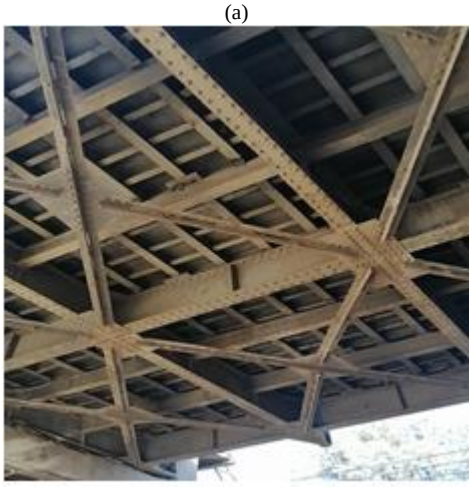

(b)

FIGURE 3. Distribution of, a) main and secondary girders, and b) bracing system and stringers

FIGURE 4. Bridge sleepers in an upright position raised for repair

Commonly, for all corroded parts sandblasting was applied prior to repair Sa2.5 [24]. For the edge beams, additional plates were welded to the deteriorated webs – certified welders conducted all welding according to Egyptian standards. The lost rivets were replaced with new firmly tight strength bolts (G10.9) of the same rivet diameter. The bearings were replaced with new ones. The local bendings among steel sections were realigned. Finally, all the refurbished parts were subjected to epoxy coating according to manufacturer recommendations. The total thickness of the coat was 360 microns – 60 microns as primer coat, 200 microns as high build coat (applied on three layers), and 120 microns of zinc rich final coat (applied on two layers). All painting was applied using a wireless technique.

(a) **(b)**

(c)

FIGURE 5. a) Corrosion**, b)** tearing, and **c)** local bending among steel movable bridge

The goal of the research was not only oriented toward the repair program but also to increase the load-carrying capacity of the bridge from 20 to 60 tons according to the ECP 2012 [25]. Moreover, the whole bridge width was utilized for traffic except 250 mm from both sides were left for side curbs. A separate newly constructed pedestrian bridge was considered as a replacement for the old sidewalks. Figure (6) shows some photos of the bridge during rehabilitation, after rehabilitation, and during the opening test. Figure (7) plane of the main system of the bridge. Figures (8-10) show sections in the bridge describing the executed strengthening.

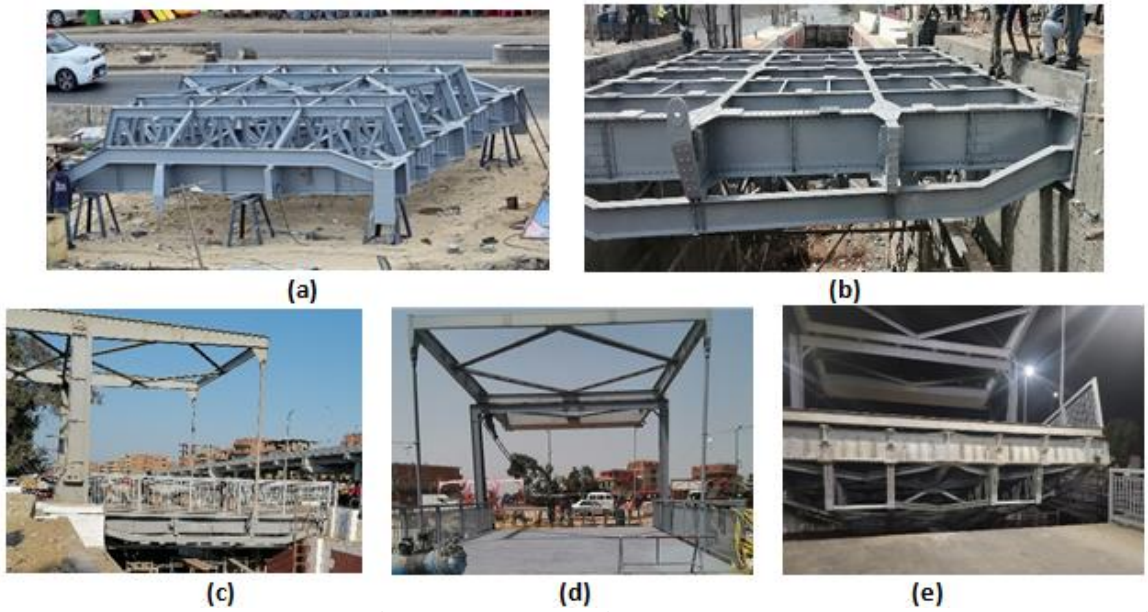

FIGURE 6. Bridge during, a) new truss system during fabrication, b) placement of strengthened bridge in desired location, c) and d) installation of all bridge components after repair, and e) bridge during opening trial test

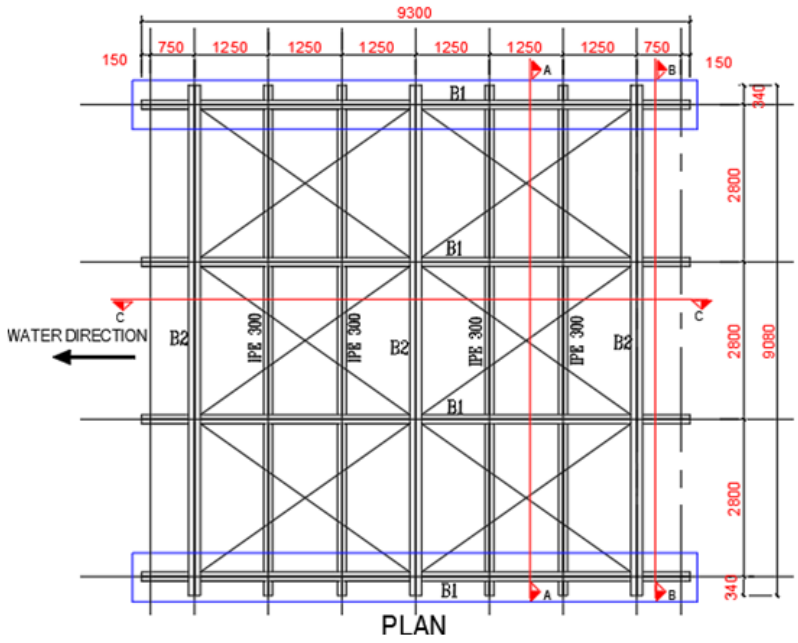

FIGURE 7. Plan of the main system of the bridge

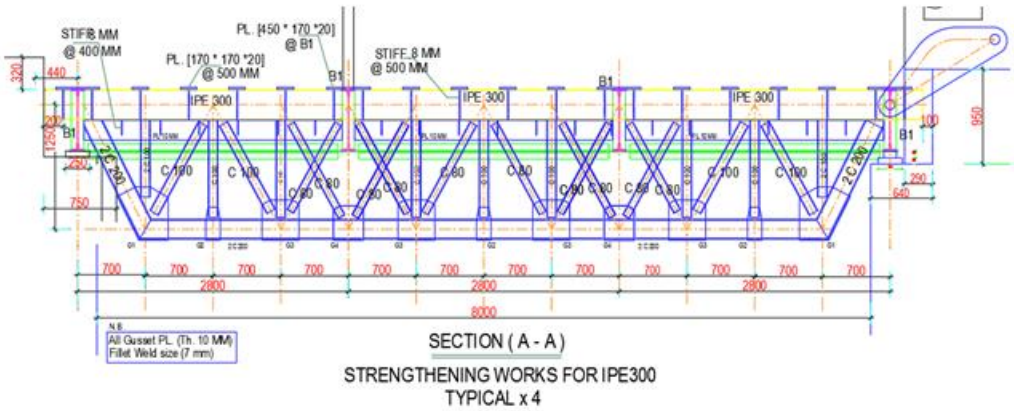

FIGURE 8. Typical strengthening of IPE300

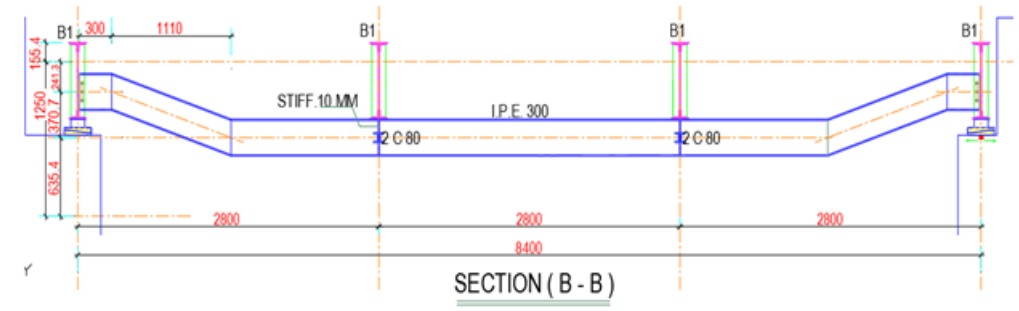

FIGURE 9. Strengthening of edge cantilever using broken beam

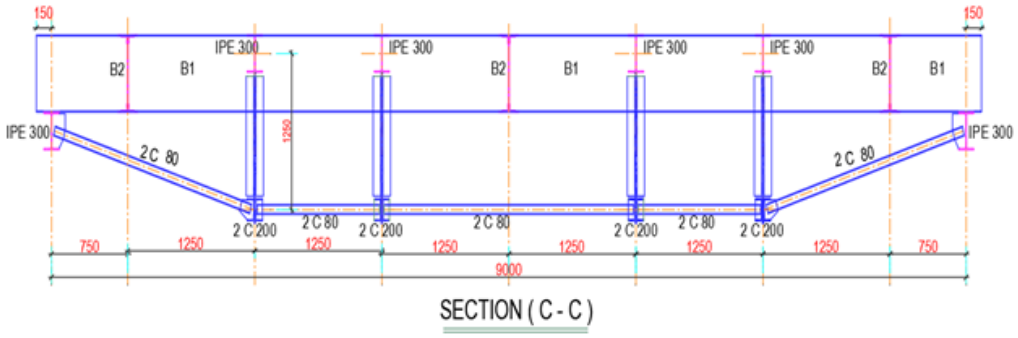

FIGURE 10. Section showing additional four trusses, two edge girders, and connecting beams

4. NUMERICAL MODELLING

Numerical analyses were conducted using four finite element models. The models were created using SAP2000 [26]. The first model (Model A) aimed to compare the internal stresses in steel sections under both the current and new desired traffic loads. Local deterioration was not considered in this level of modeling. In this model, thin shell elements were used to simulate all the main and secondary girders. The stringers were not modeled, but their loads as well as the bridge loads were transferred directly to the main statical system of the bridge. The simulation considered a lane width of 3.0 m. The weight of each vehicle was divided into two axes with four wheels as per ECP 2012 [25]. The second model (Model B) was the same as the first one but after incorporating the rehabilitation works. In this model frame elements were added to simulate additional truss members. The model helped in determining the flow of forces among new and old bridge systems and corresponding internal stresses. The model was also used for the optimum design of the truss system. The third model (Model C) was a simplified model necessary for dynamics analysis; the model was used to determine the mode shapes and fundamental frequencies before and after strengthening. In this model, only frame elements were used to represent all members of the bridge. Moreover, the modal analysis was performed considering only the original mass of the bridge. The live load was not simulated in this case. In fact, (Models A and B) were not utilized for dynamic analysis because of the large number of the existing degrees of freedom of the models. This could allow the excitation of a lot of local modes. The last model (Model D) utilized frame elements to study the bridge during lifting. The purpose of this model was to determine the straining actions among the lifting system and the required gap distance necessary for rotating the bridge without colliding with the abutment. The model was also helpful in determining the required counterweight necessary to start the movement of the strengthened bridge. Figure (11) shows the used numerical models. For all models, typical steel properties were used, Modulus of elasticity was taken 2.1x105 MPa, unit mass of 7.85 t/m3, and Poisson ratio of 0.3. Linear analysis was conducted for all models. The dead load of the main bridge system was automatically calculated from members' unit mass. Whereas flooring and weight of stringers were manually defined and distributed for all models. The obtained results were due to combinations of both dead and live loads.

4.1 Results of Numerical Modelling

Initially, (Model A) was loaded with the original traffic loads (20 tons) as well as the new desired loads (60 tons), and the straining actions were compared. The principal stresses were studied for each case. It was shown that the bridge in its current deteriorated condition might not even bear the original designed load. Thus, (Model B) was then used to simulate the strengthened bridge. The model was used to check strengthening efficiency and deduction in stresses released from the original system. Figures (12a-d) show the resulting principal stresses from these models. It was observed that the obtained principal stresses exceeded the allowable limits for the main girder and IPE300, 260, and 300 MPa were obtained, respectively. Table (1) shows a summary of the obtained stresses from Models (A) and (B). It was noticed that the decrement in the applied stress ranged from (63 – 93%) due to the strengthening effect.

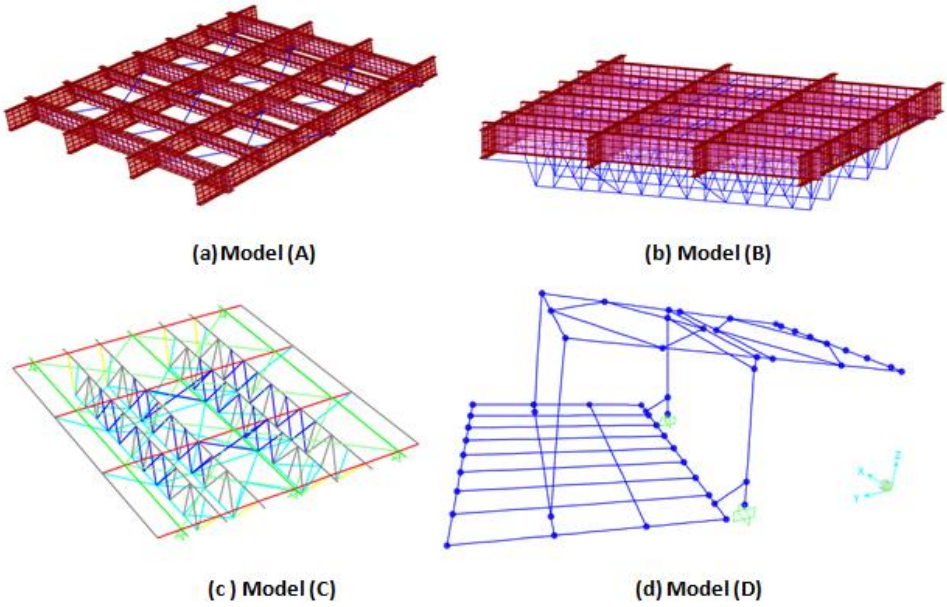

FIGURE 11. Numerical models used in the study**; a)** original state of bridge**), b)** strengthened state of bridge, **c)** simplified model for dynamic analysis, and **d)** lifting mechanism

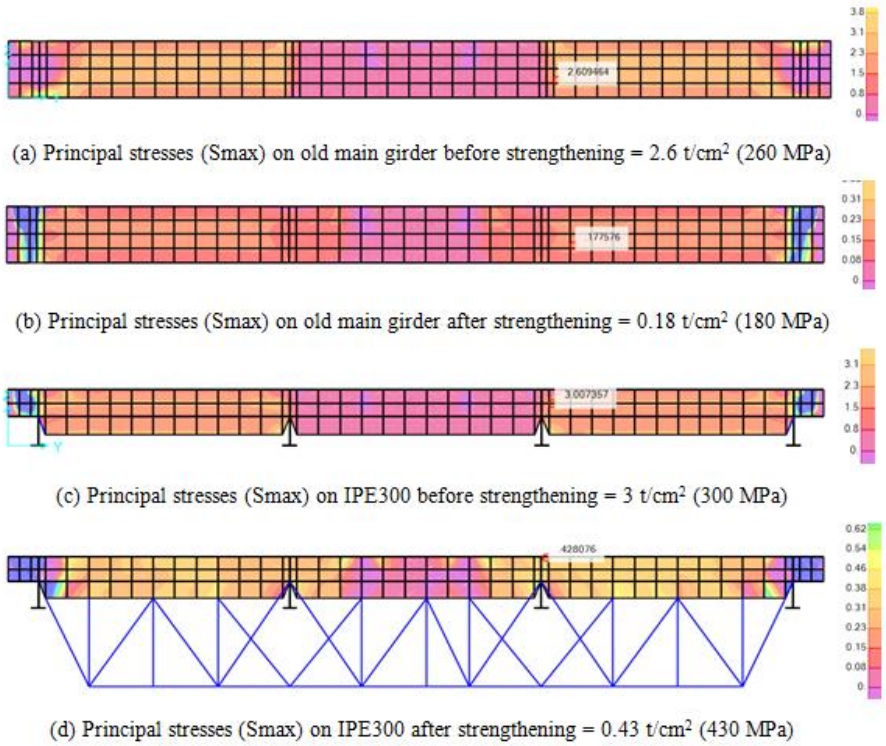

FIGURE 12. Sample of the obtained results numerically for both main and secondary beams at original and strengthened conditions

Additionally, modal analysis was conducted using the simplified Model (C). Frame elements were used to represent the main carrying system of the bridge. The simplified model presented the bridge main system only without any additional masses as the stringers and hangers were removed during the experimental dynamic test. The model was replicated twice; one represented the original state of the bridge while the other presented the strengthened state. The first dominant six modes were determined. Figures (13 and 14) show the dominant modes for the original and strengthened systems, respectively. The figures indicate that however, an increase in the overall mass of the strengthened bridge, its fundamental frequency exhibited an increase of 59% over the original bridge state. The first bending mode frequency was raised from 14.42 Hz to 22.86 Hz. This also indicated good enhancement in the structural static stiffness of the bridge after strengthening.

TABLE 1. Principal stresses among bridge elements due to a combination of dead and live loads

Location	Principal tensile stress – Smax ($x10^2$ MPa)		Principal compressive stress - Smin ($x10^2$ MPa)		% decrease in stress (Smax)	% decrease in stress (Smin)
	Old system alone	New System	Old system alone	New System		
Mid. M.G.	2.60	0.18	-1.92	-0.23	93.07	88.02
IPE300	3.00	0.43	-0.90	-0.33	85.67	63.33

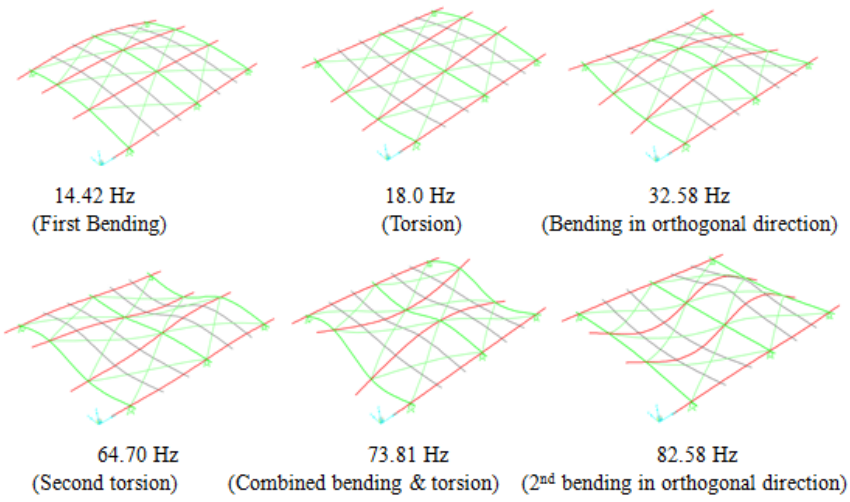

FIGURE 13. Mode shapes from numerical modeling for the original system

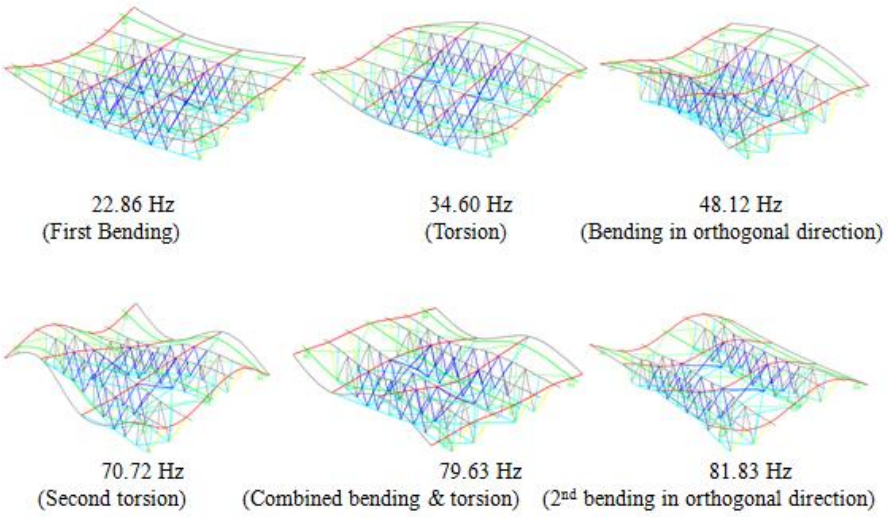

FIGURE 14. Mode shapes from numerical modeling for the strengthened system

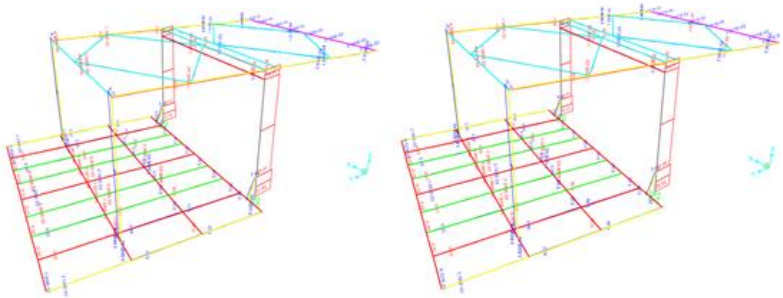

FIGURE 15. Normal force diagrams for the bridge before and after strengthening

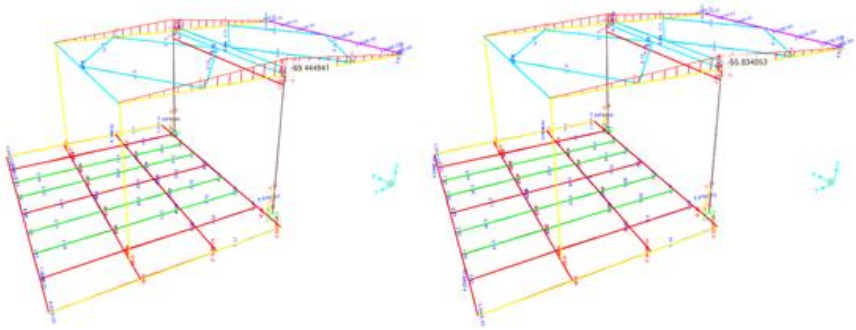

FIGURE 16. Bending moment diagram for the bridge before and after strengthening

The last model aimed to study the straining actions of the lifting mechanism, especially at the time when lifting starts. The straining actions on the cantilevers, hangers, and main columns were studied for the bridge in its original and strengthened condition. Model (D) was also used in determining the new counter mass for the strengthened bridge. The counterweight should be adjusted so that no bending moment should transfer to the columns. Figures (15 and 16) show the obtained normal force and bending moments diagrams, for both systems, respectively. A summary of the important results is shown in Table 2. It was noticed that the percentage increase in the applied straining actions due to additional mass resulted from strengthening ranges from (21 to 26 %).

The model ended up with requirements to strengthen the two cantilever girders, add bracing to the columns, and increase the lumped counter mass by 4.0 tons. It was noted that the hanger did not require any strengthening. The hanger was of a pipe cross-sectional area with an effective area of 34.5 cm^2 and a corresponding tensile capacity of 48 tons.

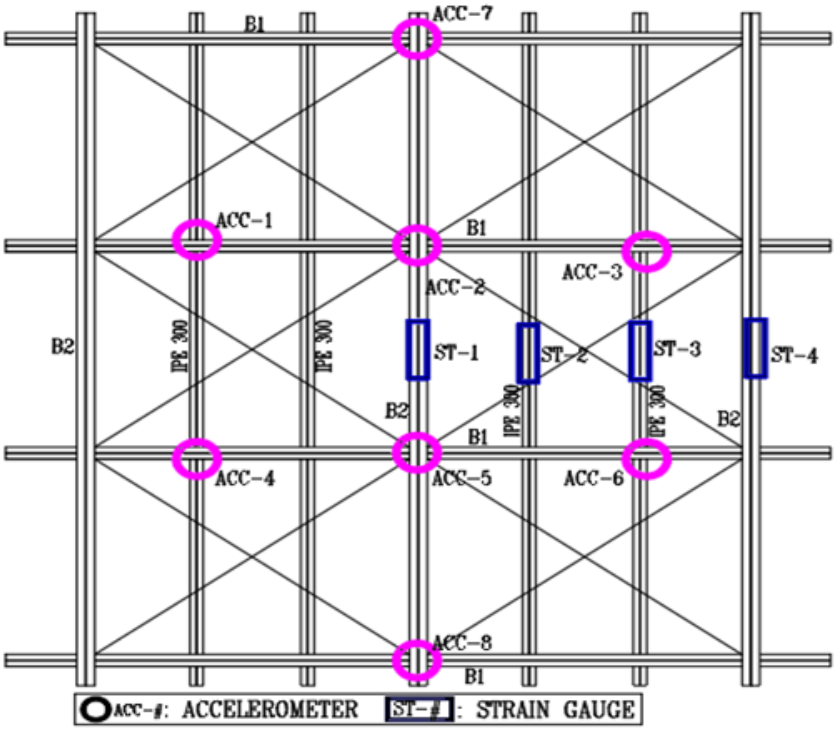

FIGURE 17. Plan showing the locations of accelerometers and strain gauges

TABLE 2. Summary of straining actions obtained from Model (D)

	Normal Force in Hanger (Ton)	Normal Force in Column (Ton)	Max. Moment at cantilever beam (Ton.m.)	Lumped counter mass (Ton mass)
Original system	+8.1	-19.3	56.3	14.0
Strengthened system (% increase)	+10.2 (25.9%)	-23.4 (21.2%)	69.2 (22.9%)	18.0 (28.6%)

5. DYNAMIC TESTING

The dynamic characteristics of the bridge were determined before and after strengthening. Eight uniaxial piezoelectric accelerometers of a resonant frequency of more than 10 kHz. were used. Line-powered signal conditioners were used to provide constant current excitation to the sensors. The acceleration time history in the vertical direction was only recorded. To capture the contribution on higher modes, particularly for strengthened bridge, as well as to obtain data with high resolution, a reasonable sampling rate of 500 Hz was used. The bridge was excited using a sludge hummer of mass (5 Kg.) and the free vibration wave was recorded just after impact. The accelerometers were mounted and distributed among the bridge as shown in Figure (17). This test can be considered as one of the non-destructive quality control tests during the rehabilitation process. The acceleration time histories of the bridge were recorded on the main carrying system of the bridge while having the deck and stringers removed. The hangers were also unattached during the test. Modal analysis was conducted, and the mode shapes and corresponding frequencies were obtained. The obtained natural frequencies were obtained and compared before and after strengthening. Figures (18 and 19) show the obtained mode shapes for both the original and strengthened system, respectively. The figures elaborate that the enhancement along the main direction of the bridge was enhanced significantly compared to the orthogonal direction. It was also depicted that the frequencies of the first and third modes – representing the first and second in-plane bending modes were increased. Whereas the frequencies of the orthogonal direction were slightly changed. It was noted that the enhancement in the natural frequency of the first bending mode for the strengthened system (22.1 Hz) was 38.12% over the corresponding value for the original system (16 Hz). For the second bending mode, the frequencies of the original and the strengthened systems were 66.9 Hz and 79.1 Hz, respectively with almost 18% increase. The obtained frequencies from field measurements agreed with their corresponding values obtained numerically. Particularly, the first dominant bending modes were so closed whereas, the difference slightly increased at higher modes. This could be attributed to difficulty in representing the exact degree of joints connectivity and supporting system.

Figures (20 and 21) show selected records for acceleration time histories for original and strengthened conditions for selected channels only. It can be noticed that for the original system, the vibration damped significantly in a shorter time compared to the strengthened system. This could be attributed to the presence of deterioration and local cracks in the original system. The new system shows a healthier condition of the bridge.

Moreover, Fast Fourier Transformation (FFT) was conducted to determine the dominant contributing frequencies for both systems. Figures (22 and 23) show FFT plots for the bridge before and after strengthening, respectively. The results were in great agreement with the mode shapes obtained through modal analysis. It can be distinguished that the FFT plot for the bridge in its original condition contains a lot of local damage which results in having a bundle of frequencies. In contrast, the efficiency of the strengthening appeared to have determined clear peaks indicating the consistency of the new bridge. The dominant frequencies in each plot were written against their corresponding peaks.

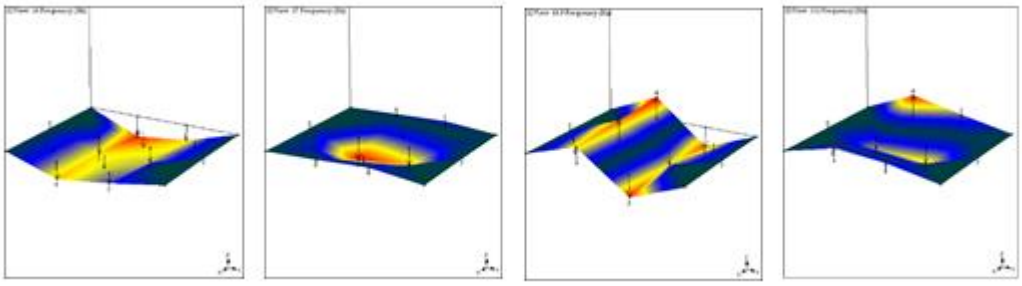

FIGURE 18. Experimental mode shapes for the original system

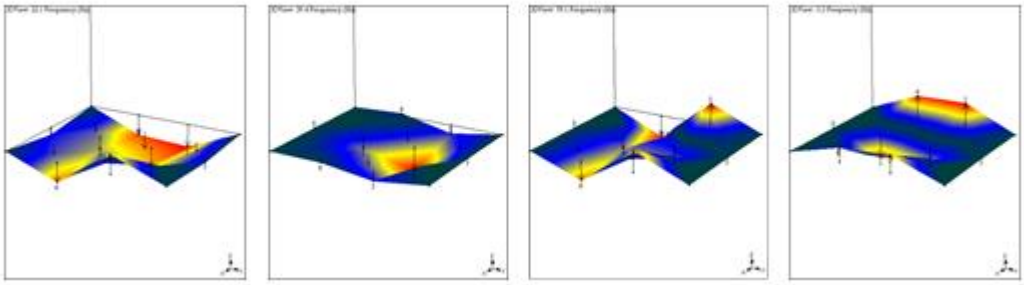

FIGURE 19. Experimental mode shapes for the strengthened system

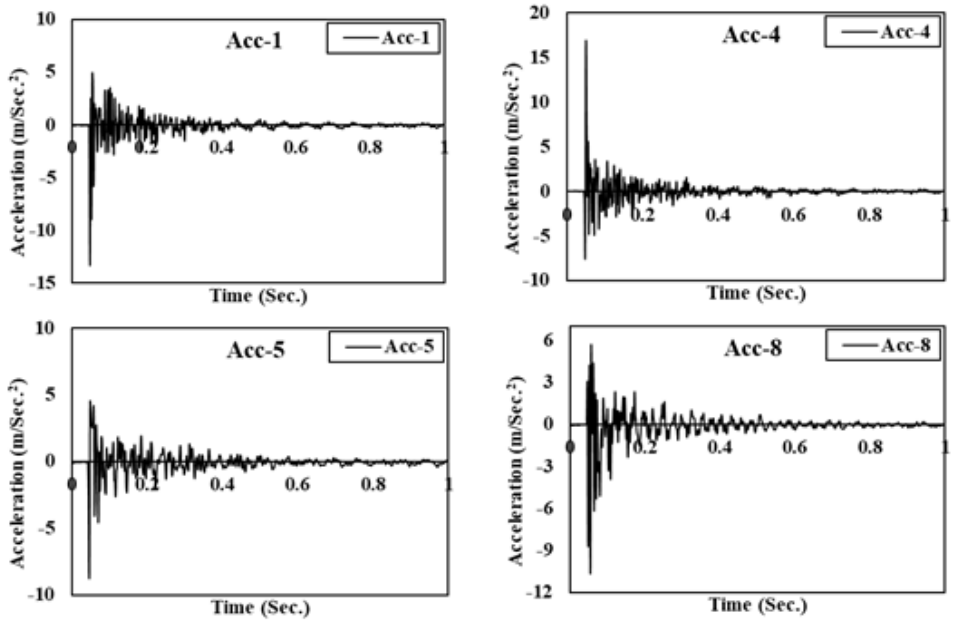

FIGURE 20. Sample of acceleration time histories before strengthening

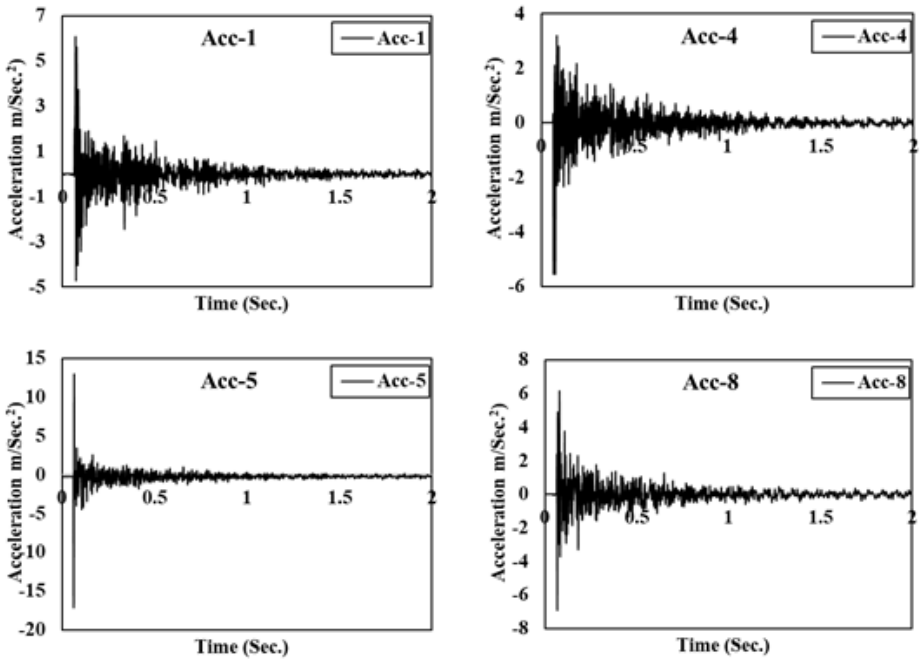

FIGURE 21. Sample of acceleration time histories after strengthening

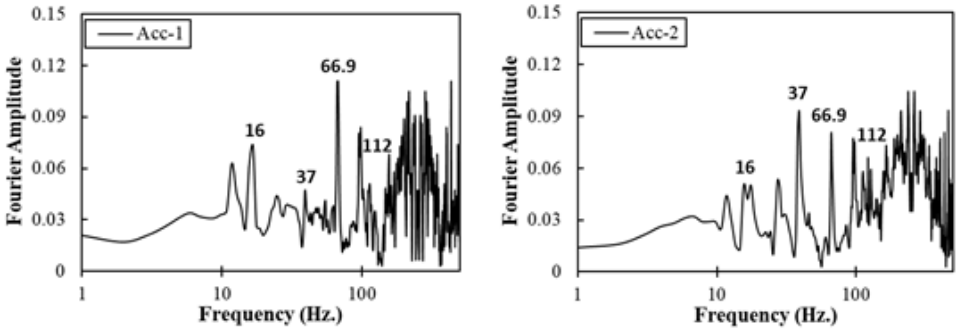

FIGURE 22. Sample of FFT before strengthening

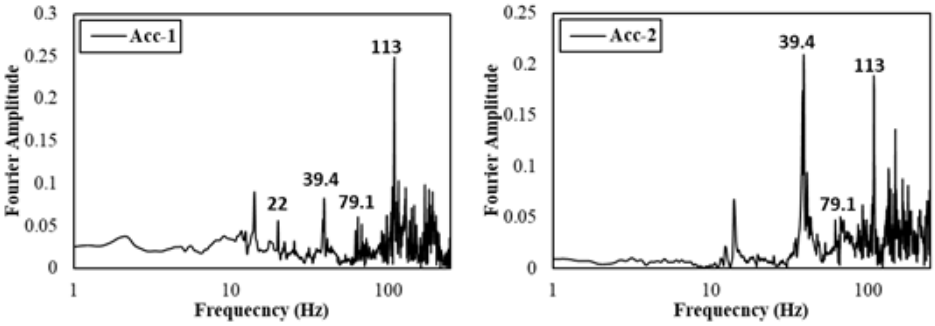

FIGURE 23. Sample of FFT after strengthening

6. DYNAMIC STRAIN MEASUREMENTS

To ensure the efficiency of the strengthened bridge, dynamic strain measurements during normal traffic loads were recorded only for the bridge after strengthening. It was noted that heavy to medium trucks of approximate weights from (8 – 40 tons) were observed along with some limousine vehicles crossing the bridge. The bridge was first emptied of all kinds of vehicles for a while and then opened for normal traffic. Four strain gauges were mounted to the soffit of the girders and trusses as per the distribution given in Figure (17). All the strain gauges were balanced, recording started, and normal flow was allowed. Several records were captured where the effect of additional strain due to live loads only was considered. Figures (24a and b) show the continuously measured strains on the old system as well as the new truss system at different recording intervals. The earlier figure shows monitoring for heavy trucks. Whereas the latter shows strain time history for medium-weight and light limousines. Table (3) shows the maximum monitored strain and corresponding stresses among the soffit of the measured elements at different portions of the strengthened system. This allowed the comparison of the level of stress exerted by different elements in the retrofitted bridge under same loading condition. Thus, the efficiency of strengthening can be noticed. It can also be observed that the strain value measured on the original girder after strengthening exerted the least strain value. This indicates the efficiency of the strengthening system and the ability of the additional trusses to reduce the stresses from the old, deteriorated bridge and transferring them to the new carrying system. It was also clear that the level of strains was closed in values regardless of the position of the trucks. This could be attributed to the efficiency of the new system in distribution of traffic loads on the bridge deck.

TABLE 3. Maximum monitored strain and corresponding stress values due to live load only for strengthened bridge

Location	Max. Measured strain (με)	Corresponding Normal stress at soffits (x100 MPa)
Strain#1: (Main girder - old system)	82	0.17
Strain#2: (new truss system)	93	0.20
Strain#3: (new truss system)	90	0.19
Strain#4: (edge beam)	100	0.21

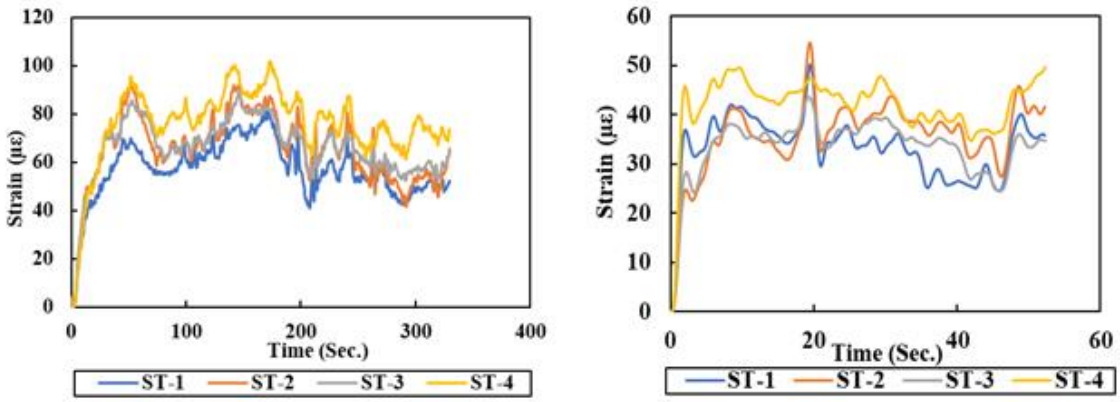

FIGURE 24. Sample of strain range after strengthening for a) heavy trucks, and b) medium-weight trucks

7. CONCLUSIONS

Upgrading the load-carrying capacity of a heritage riveted steel bridge, from 20 to 60 tons, was addressed in this research. A real case study was explored. This was a part of a full rehabilitation program conducted on an ancient regulator with an attached steel bridge. Conventional repair as well as developing of new truss to support the original bridge in carrying the new loads. Evaluation of the strengthened bridge was conducted with the aid of vibration analysis and operational dynamic strain measurements. The following were among the main findings of the research:

1- Despite having an extra mass due to adding a new truss system, numerical results showed an overall reduction in the principal stresses among original bridge members between (63 – 93%). The same range of stresses was also measured in the field. This also ensures good agreement between numerical and physical applications indicating good efficiency of the proposed strengthening.

2- The processing of measured acceleration time history before and after strengthening showed an increase in the fundamental natural frequency of the bridge. The frequency of the dominant first bending mode was increased by 38% after strengthening.

3- Due to random traffic monitoring, a range of stresses was estimated (170 – 210 MPa) due to normal operational live loads only. This indicates that the bridge followed the correct design and construction criteria.

References

[1] C. Cui, Q. Zhang, D. Zhang, W. Lao, L. Wu, and Z. Jiang, ‘Monitoring and detection of steel bridge diseases: A review’, Journal of Traffic and Transportation Engineering (English Edition), vol. 11, no. 2, pp. 188–208, Apr. 2024, doi: 10.1016/j.jtte.2024.03.001.

[2] B. J. A. Costa and J. A. Figueiras, ‘Rehabilitation and condition assessment of a centenary steel truss bridge’, J Constr Steel Res, vol. 89, pp. 185–197, 2013, doi: 10.1016/j.jcsr.2013.06.013.

[3] C. S. Horas, J. N. Silva, J. A. F. O. Correia, and A. M. P. De Jesus, ‘Fatigue damage assessment on aging riveted metallic railway bridges: A literature review’, Structures, vol. 58, p. 105664, Dec. 2023, doi: 10.1016/j.istruc.2023.105664.

[4] Dorin Radu, Radu Băncilă, Simon Sedmak, and Mihajlo Aranđelović, ‘Residual life of a historic riveted steel bridge - engineering critical assessment approach’, Procedia Structural Integrity, vol. 42, pp. 1106–1112, 2022.

[5] G. Alencar, A. de Jesus, J. G. S. da Silva, and R. Calçada, ‘Fatigue cracking of welded railway bridges: A review’, Eng Fail Anal, vol. 104, pp. 154–176, Oct. 2019, doi: 10.1016/j.engfailanal.2019.05.037.

[6] J. M. Pardal et al., ‘Failure characterization of a structural welded component of an ancient bridge’, Eng Fail Anal, vol. 116, p. 104751, Oct. 2020, doi: 10.1016/j.engfailanal.2020.104751.

[7] H. Ren, Z. Fu, B. Ji, and Z. Zhang, ‘Evaluation of stability behavior of the steel truss-arch composite structure’, Structures, vol. 57, p. 105240, Nov. 2023, doi: 10.1016/j.istruc.2023.105240.

[8] A. L. L. Silva et al., ‘Fatigue strength assessment of riveted details in railway metallic bridges’, Eng Fail Anal, vol. 121, p. 105120, Mar. 2021, doi: 10.1016/j.engfailanal.2020.105120.

[9] M. Mashayekhi and E. Santini-Bell, ‘Fatigue assessment of a complex welded steel bridge connection utilizing a three-dimensional multi-scale finite element model and hotspot stress method’, Eng Struct, vol. 214, p. 110624, Jul. 2020, doi: 10.1016/j.engstruct.2020.110624.

[10] X. Jiang, Z. Lv, X. Qiang, and S. Song, ‘Fatigue performance improvement of U-rib butt-welded connections of steel bridge decks using externally bonded CFRP strips’, Thin-Walled Structures, vol. 191, p. 111017, Oct. 2023, doi: 10.1016/j.tws.2023.111017.

[11] M. Monteiro, V. Brito, and T. Mendonça, ‘Tagus river centenarian steel bridges’ rehabilitation’, Procedia Structural Integrity, vol. 5, pp. 48–54, 2017, doi: 10.1016/j.prostr.2017.07.061.

[12] J. A. Mash, K. A. Harries, and C. Rogers, ‘Repair of corroded steel bridge girder end regions using steel, concrete, UHPC and GFRP repair systems’, J Constr Steel Res, vol. 207, p. 107975, Aug. 2023, doi: 10.1016/j.jcsr.2023.107975.

[13] Z. Lv, X. Jiang, X. Qiang, and W. Chen, ‘Proactive strengthening of U-rib butt-welded joints in steel bridge decks using adhesively bonded Fe-SMA strips’, Eng Struct, vol. 301, p. 117316, Feb. 2024, doi: 10.1016/j.engstruct.2023.117316.

[14] X. Qiang, Y. Wu, Y. Wang, and X. Jiang, ‘Novel crack repair method of steel bridge diaphragm employing Fe-SMA’, Eng Struct, vol. 292, p. 116548, Oct. 2023, doi: 10.1016/j.engstruct.2023.116548.

[15] A. Hosseini, E. Ghafoori, R. Al-Mahaidi, X.-L. Zhao, and M. Motavalli, ‘Strengthening of a 19th-century roadway metallic bridge using nonprestressed bonded and prestressed unbonded CFRP plates’, Constr Build Mater, vol. 209, pp. 240–259, 2019, doi: 10.1016/j.conbuildmat.2019.03.095.

[16] E. Ghafoori, A. Hosseini, R. Al-Mahaidi, X.-L. Zhao, and M. Motavalli, ‘Prestressed CFRP-strengthening and long-term wireless monitoring of an old roadway metallic bridge’, Eng Struct, vol. 176, pp. 585–605, 2018, doi: 10.1016/j.engstruct.2018.09.042.

[17] Lars Sieber, Ralf Urbanek, and Jurgen Bar, ‘Crack-Detection in old riveted steel bridge structures’, Procedia Structural Integrity, vol. 17, pp. 339–346, 2019.

[18] A. Bayraktar, A. C. Altunişik, and T. Türker, ‘Structural health assessment and restoration procedure of an old riveted steel arch bridge’, Soil Dynamics and Earthquake Engineering, vol. 83, pp. 148–161, Apr. 2016, doi: 10.1016/j.soildyn.2016.01.012.

[19] B. Torres, P. Poveda, S. Ivorra, and L. Estevan, ‘Long-term static and dynamic monitoring to failure scenarios assessment in steel truss railway bridges: A case study’, Eng Fail Anal, vol. 152, p. 107435, Oct. 2023, doi: 10.1016/j.engfailanal.2023.107435.

[20] B. Barros, B. Conde, M. Cabaleiro, and B. Riveiro, ‘Design and testing of a decision tree algorithm for early failure detection in steel truss bridges’, Eng Struct, vol. 289, p. 116243, Aug. 2023, doi: 10.1016/j.engstruct.2023.116243.

[21] J. Kafie-Martinez, P. B. Keating, P. Chakra-Varthy, J. Correia, and A. de Jesus, ‘Stress distributions and crack growth in riveted lap joints fastening thick steel plates’, Eng Fail Anal, vol. 91, pp. 370–381, Sep. 2018, doi: 10.1016/j.engfailanal.2018.04.048.

[22] J. A. Mash and K. A. Harries, ‘Numeric simulation of corroded steel bridge girder end region repairs’, J Constr Steel Res, vol. 210, p. 108048, Nov. 2023, doi: 10.1016/j.jcsr.2023.108048.

[23] A. Sedmak, D. Radu, M. Aranđelović, S. Sedmak, and R. Băncilă, ‘Residual life assessment of the historical road riveted bridges’, Eng Fract Mech, vol. 299, p. 109960, Mar. 2024, doi: 10.1016/j.engfracmech.2024.109960.

[24] ISO 8501-1:2007(R 2011) Preparation of steel substrates before application of paints and related products -- Visual assessment of surface cleanliness -- Part 1: Rust grades and preparation grades of uncoated steel substrates and of steel substrates after overall removal of previous coatings

[25] ECP- Mistrial decree (431), Egyptian Code for Calculating Loads and Forces on Structural and Masonry Works, 2012th ed. 2011.

[26] ‘SAP2000, CSI: Computers and Structures Inc, Version 14.1.0. Computer software, 2009.’